Black Carbon Involved Photochemistry Enhances the Formation of Sulfate in the Ambient Atmosphere: Evidence from in-situ Individual Particle Investigation

Guohua Zhang[1], Yuzhen Fu[1], Xiaocong Peng[1], Wei Sun[1], Zongbo Shi[2], Wei Song[1], Weiwei Hu[1], Duohong Chen[3], Xiufeng Lian[1], Lei Li[4], Mingjin Tang[1], Xinming Wang[1], and Xinhui Bi[1]

[1]Guangzhou Institute of Geochemistry, Chinese Academy of Sciences
[2]University of Birmingham
[3]Guangdong Environmental Monitoring CenterGuangzhouChina
[4]Institute of Mass Spectrometer and Atmosphere Environment, Jinan University

November 23, 2022

Abstract

Mixing state of black carbon (BC) with secondary species has been highlighted as a major uncertainty in assessing its radiative forcing. While recent laboratory simulation has demonstrated that BC could serve as a catalyst to enhance the formation of sulfate, its role in the formation and evolution of secondary aerosols in the real atmosphere remains poorly understood. In the present study, the mixing of BC with sulfate/nitrate in the atmosphere of Guangzhou (China) was directly investigated with a single particle aerosol mass spectrometer (SPAMS). The peak area ratios of sulfate to nitrate (SNRs) for the BC-containing particles are constantly higher than those of the BC-free particles (with negligible BC signals). Furthermore, the seasonal SNR peak is observed in summer and autumn, and the diurnal peak is found in the afternoon, consistent with the trends of radiation-related parameters (i.e., solar radiation and temperature), pointing to the BC-induced photochemical production of sulfate. Such hypothesis is further supported by the multilinear regression and random forest analysis, showing that the variation of SNRs associated with the BC-containing particles could be well explained ($R^2 = $ ~0.7-0.8) by the radiation-related parameters ($> 30\%$ of the variance) and the relative BC content (~20%) in individual particles, but with limited influence of precursors (SO_2/NO_x: $< 5\%$). Differently, the radiation-related factors only explain $< 10\%$ of the SNR variation for the BC-free particles. These results provide ambient observational evidence pointing to a unique role of BC on the photochemical formation and evolution of sulfate, which merits further quantitative evaluations.

Hosted file

si for bc particles.docx available at https://authorea.com/users/542068/articles/600810-black-carbon-involved-photochemistry-enhances-the-formation-of-sulfate-in-the-ambient-atmosphere-evidence-from-in-situ-individual-particle-investigation

1   **Black Carbon Involved Photochemistry Enhances the Formation of Sulfate in the**

2   **Ambient Atmosphere: Evidence from *in-situ* Individual Particle Investigation**

3

4   Guohua Zhang[1,2,3,*], Yuzhen Fu[1,2,4], Xiaocong Peng[1,2,4], Wei Sun[1,2,4], Zongbo Shi[5], Wei

5   Song[1,2,3], Weiwei Hu[1,2,3], Duohong Chen[6], Xiufeng Lian[7], Lei Li[7], Mingjin Tang[1,2,3], Xinming

6   Wang[1,2,3], Xinhui Bi[1,2,3,*]

7

8   [1] State Key Laboratory of Organic Geochemistry and Guangdong Provincial Key Laboratory

9   of Environmental Protection and Resources Utilization, Guangzhou Institute of Geochemistry,

10 Chinese Academy of Sciences (CAS), Guangzhou 510640, PR China

11 [2] CAS Center for Excellence in Deep Earth Science, Guangzhou, 510640, China

12 [3] Guangdong-Hong Kong-Macao Joint Laboratory for Environmental Pollution and Control,

13 Guangzhou Institute of Geochemistry, CAS, Guangzhou 510640, PR China

14 [4] University of Chinese Academy of Sciences, Beijing 100049, PR China

15 [5] School of Geography, Earth and Environmental Sciences, University of Birmingham,

16 Birmingham B15 2TT, U.K.

17 [6] State Environmental Protection Key Laboratory of Regional Air Quality Monitoring,

18 Guangdong Environmental Monitoring Center, Guangzhou 510308, PR China

19 [7] Institute of Mass Spectrometer and Atmospheric Environment, Jinan University, Guangzhou

20 510632, PR China

21

22 *Corresponding to Guohua Zhang (zhanggh@gig.ac.cn) and Xinhui Bi (bixh@gig.ac.cn)

23

Abstract

Mixing state of black carbon (BC) with secondary species has been highlighted as a major uncertainty in assessing its radiative forcing. While recent laboratory simulation has demonstrated that BC could serve as a catalyst to enhance the formation of sulfate, its role in the formation and evolution of secondary aerosols in the real atmosphere remains poorly understood. In the present study, the mixing of BC with sulfate/nitrate in the atmosphere of Guangzhou (China) was directly investigated with a single particle aerosol mass spectrometer (SPAMS). The peak area ratios of sulfate to nitrate (SNRs) for the BC-containing particles are constantly higher than those of the BC-free particles (defined as particles with negligible BC signals). Furthermore, the seasonal SNR peak is observed in summer and autumn, and the diurnal peak is found in the afternoon, consistent with the trends of radiation-related parameters (i.e., solar radiation and temperature), pointing to the BC-induced photochemical production of sulfate. Such hypothesis is further supported by the multilinear regression and random forest analysis, showing that the variation of SNRs associated with the BC-containing particles could be well explained (R^2 = ~0.7-0.8) by the radiation-related parameters (> 30% of the variance) and the relative BC content (~20%) in individual particles, but with limited influence of precursors (SO_2/NO_x: < 5%). Differently, the radiation-related factors only explain < 10% of the SNR variation for the BC-free particles. These results provide ambient observational evidence pointing to a unique role of BC on the photochemical formation and evolution of sulfate, which merits further quantitative evaluations.

Keywords: black carbon; sulfate; individual particles; mixing state; SPAMS

45   **Key points:**

46   1. Enhanced sulfate to nitrate ratios (SNRs) are observed for the BC-containing particles

47   2. The distinct diurnal variation of the enhanced SNRs is most likely attributed to BC catalytic

48   photochemistry

49   3. SNRs in individual BC-containing particles could be well predicted by the radiation-related

50   parameters and the relative BC content

1 Introduction

As a substantial fraction of atmospheric aerosols, black carbon (BC) or soot enhances haze pollution, modifies the regional meteorology, and imposes a tremendous positive forcing on the global climate by absorbing solar radiation [*Bond et al.*, 2013; *Ding et al.*, 2016; *Penner*, 2019]. While freshly emitted BC contains limited coating, atmospheric aging such as coagulation with other particles, condensation of vapors, and cloud processing will lead to internally mixed BC particles with complex compositions [*Zhang et al.*, 2018; *Riemer et al.*, 2019]. These aging processes result in considerable variability in morphology, mixing state, and hygroscopic and optical properties of BC particles, subsequently leading to the modification of climatic and health effects [*Zhang et al.*, 2008; *He et al.*, 2015; *Peng et al.*, 2016]. Nevertheless, significant discrepancies between standard model predictions and regionally-specific observations are tightly related to distinct compositional heterogeneity (or mixing state) among BC particles [*Liu et al.*, 2017; *Matsui et al.*, 2018; *Fierce et al.*, 2020].

As one of the most critical factors determining the absorption of BC, the mixing state of individual BC particles is highly complicated and constantly changing during their transport in the atmosphere. BC particles were observed to be extensively internally mixed worldwide [*Adachi et al.*, 2016; *Liu et al.*, 2017; *Zhang et al.*, 2017; *Motos et al.*, 2019], including various areas around China, such as the Pearl River Delta (PRD) region [*Huang et al.*, 2012; *Zhang et al.*, 2014; *Tan et al.*, 2016], Yangtze River Delta region [*Kleffmann and Wiesen*, 2005], and North China Plain [*Cheng et al.*, 2009; *Zhang et al.*, 2018; *Yu et al.*, 2020], leading to significantly enhanced light scattering and absorption capacity of BC. While extensive studies

have gained insight into the evolution of mixing state of BC particles, it has been merely linked

to the condensation of secondary species, such as sulfate, nitrate, and organics [*Cahill et al.*,

2012; *Zhang et al.*, 2013; *Zhang et al.*, 2018; *Yuan et al.*, 2019]. Actually, BC can be actively

involved in the formation of secondary species, through interacting with atmospheric reactive

species, such as NO_2, SO_2, O_3, and HNO_3 [*Kleffmann and Wiesen*, 2005; *McCabe and Abbatt*,

2009; *Khalizov et al.*, 2010; *Han et al.*, 2013b; *Zhao et al.*, 2017]. A recent laboratory study

indicates that the BC catalytic chemistry should play a considerable role in the enhanced sulfate

formation during the regional haze in China, in the presence of ammonia and NO_2 [*Zhang et

al.*, 2020]. Besides, the photochemical oxidation of some intrinsic organic compositions by O_2

might also be an essential aging process for BC [*Han et al.*, 2012]. There is also growing

evidence demonstrating that BC is photoactive and could release reactive oxygen species (ROS)

including $^1O_2$ and $\cdot OH$, which may represent a crucial aging pathway of BC [*Gehling and

Dellinger*, 2013; *Li et al.*, 2018b; *Li et al.*, 2019].

Despite environmental significance, whether the intrinsic properties of BC particles are

significant in the formation and evolution of secondary compositions in the ambient atmosphere

remains poorly understood. The main challenge to address such issues in field measurement is

to track the heterogeneous reactions unique to the BC-containing particles, which relies on

individual particle techniques accompanied with chemical information. For instance, with an

Aerodyne soot particle - aerosol mass spectrometer (SP-AMS), various non-refractory species

(e.g., sulfate, nitrate, and organics) associated with refractory BC can be quantitatively traced

in real-time [*Lee et al.*, 2015; *Wang et al.*, 2016b]. The temporal variation of secondary

93 compositions internally mixed with BC could also be indicated by single-particle mass

94 spectrometry (SPMS), despite only semi-quantitative information obtained [*Cahill et al.*, 2012;

95 *Healy et al.*, 2012; *Zhang et al.*, 2014]. Measurements with both techniques have indicated that

96 active photochemical formation of oxidized organics and sulfate could lead to a distinct diurnal

97 circle of mixing state of BC-containing particles. However, the role of BC in such chemistry

98 has not been identified yet. In addition, there is still a lack of treatments for heterogeneous

99 reactions on different types of particles in most models [*Zheng et al.*, 2015]. Therefore, it is

100 necessary to comprehensively evaluate the effect of heterogeneous chemistry involving BC

101 particles on the formation of secondary compositions.

102   In the present study, a Single Particle Aerosol Mass Spectrometer (SPAMS) was applied

103 to measure the size and chemical compositions of individual particles, in order to accommodate

104 the specific role of BC in the formation of secondary species. The variation of sulfate (with

105 nitrate as a reference) associated with both the BC-containing and BC-free particles, and also

106 their diurnal trends, are analyzed and discussed. The main objectives are (1) to verify whether

107 BC regulates the formation and evolution of sulfate in the ambient atmosphere and (2) to

108 explore the dependence of sulfate production on atmospheric conditions, including their

109 precursors and meteorological parameters.

110 **2 Methods**

111 **2.1 Data collection**

112   On-line measurements were conducted at a representative urban site in Guangzhou (China)

113 [*Zhang et al.*, 2019a], a megacity in the PRD region. The measurements cover four seasons,

114   including spring (21/02 to 11/04, 2014), summer (13/06 to 16/07, 2013), autumn (26/09 to 19/10,

115   2013), and winter (15/12 to 25/12, 2013). The sampling inlet for fine particle characterization

116   was situated ~40 meters above the ground level.

117   The size and chemical composition of dried individual particles were obtained by the

118   SPAMS (Hexin Analytical Instrument Co., Ltd., China) in real-time [*Li et al.*, 2011]. Briefly,

119   particles are introduced into the SPAMS through a critical orifice. They are focused and

120   accelerated to specific velocities determined by two diode Nd:YAG laser beams (532 nm)

121   located 6 cm apart. Based on the measured velocities, a pulsed laser (266 nm) downstream can

122   be triggered to desorb/ionize these individual particles, and ion fragments were produced and

123   measured by a time-of-flight mass spectrometer. As a result, velocity, detection moment, and

124   mass spectrum for each ionized particle are recorded. The velocity could be converted to

125   vacuum aerodynamic diameter (d_{va}) based on a calibration function created using polystyrene

126   latex spheres (PSL, Duke Scientific Corp., Palo Alto) with predefined sizes.

127   The auxiliary meteorological data, including ambient temperature (T), relative humidity

128   (RH) and wind speed (WS), and concentration of gaseous pollutants (SO_2, NO_x, and O_3), BC,

129   and $PM_{2.5}$, provided by Guangdong Environmental Monitoring Center, are shown as diurnal

130   trends in Fig. S1 (Supporting Information).

131   **2.2 Data analysis**

132   **2.2.1 SPAMS Data**

133   BC-containing particles are classified according to the relative peak area (RPA) of carbon

134   ion cluster (i.e., m/z ±12[C]$.^{+/-}$, ±36[C$_3$]$.^{+/-}$, ±48[C$_4$]$.^{+/-}$ or ±60[C$_5$]$.^{+/-}$), which is set as larger

135   than 0.05. And thus, particles with RPA < 0.05 are regarded as BC-free particles. The potential

136   influence of the arbitrarily defined RPA for BC screening on the conclusions is also evaluated

137   in section 3.4. Defined as the peak area of each m/z divided by the total ion mass spectral peak

138   areas, RPA is generally applied to indicate the relative fraction of a single species in individual

139   particles [*Gross et al.*, 2000]. The BC-containing particles ruled out with such criteria account

140   for ~60-80% of all the measured particles (Table S1), which are in the range of those reported

141   in the urban atmosphere [*Healy et al.*, 2013].

142   The majority of the measured BC-containing particles distribute in a size range of 0.2–1.0

143   μm (Fig. S2a), generally consistent with their dominant mass fraction in the atmosphere of the

144   PRD region [*Huang et al.*, 2012]. Representative ion peaks for the BC-containing particles, as

145   presented in Fig. S2b, are carbon ion cluster (e.g., m/z $\pm12[C]^{+/-}$, $\pm36[C_3]^{+/-}$, $\pm48[C_4]^{+/-}$ and

146    $\pm60[C_5]^{+/-}$), organic carbon (OC) fragments (m/z $27[C_2H_3]^+$, $29[C_2H_5]^+$, $37[C_3H]^+$, $26[CN]^-$,

147    $42[CNO]^-$, and $43[C_2H_3O]^+$), and secondary inorganic species, such as sulfate ($-97[HSO_4]^-$),

148   nitrate ($-62[NO_3]^-$), and ammonium ($18[NH_4]^+$). There are also some metallic species such as

149    $23[Na]^+$ and $39[K]^+$.

150   In the present study, we mainly focus on the difference of sulfate to nitrate ratio (SNR)

151   between the BC-containing and BC-free particles. The respective RPA ratios of sulfate and

152   nitrate between the BC-containing and BC-free particles were compared over the seasons, as

153   shown in Fig. S3. These ratios show significant variations, with higher values for sulfate RPA

154   ratios and lower values for nitrate RPA ratios in the BC-containing particles, indicating a

155   relatively higher fraction of sulfate rather than nitrate in these particles. It is also noted that the

156 sulfate RPAs are lower for the BC-containing particles than the BC-free particles, which is

157 likely attributable to the matrix effect during the ionization. And thus, only the SNR is applied

158 to make it comparable between the BC-containing and BC-free particles.

159 **2.2.2 Multiple linear and random forest regression**

160 Multiple linear and random forest analysis, explicitly describing a relationship between

161 predictor and response variables (i.e., regressors) [*Berk*, 2008], are applied to estimate the

162 relative contribution of several factors to the variations of SNRs for the BC-containing and BC-

163 free particles, respectively. In the multiple linear models, the least-squares fit is used, and two

164 of the most common measures of model fit are the residual standard error and the proportion of

165 variance explained (R^2). Furthermore, the Relaimpo package is used to assess the relative

166 importance of regressors in the linear model and offers the possibility of bootstrapping them

167 [*Groemping*, 2006]. Differently, random forest is for nonlinear multiple regression and has been

168 widely applied for prediction and classification, using trees as building blocks to construct

169 powerful prediction models [*Breiman*, 2001]. The algorithm first creates multiple decision trees,

170 where each tree is grown by using the bootstrap re-sampling method. The relative importance

171 of the predictor variables can also be obtained, with "Mean Decrease Accuracy" presenting the

172 capability of each independent variable in explaining the variability of SNRs.

173 **3 Results and Discussion**

174 **3.1 Distinct variations of SNR associated with the BC-containing particles**

175 As can be seen in Fig. 1, the variations of SNR are distinguished between the BC-

176 containing and BC-free particles. The SNR shows an apparent seasonal variation, with higher

177 values in summer and autumn but lower in spring and winter. Despite the similar SNR

178 variations for both particle types over the seasons, the SNRs in the BC-containing particles are

179 obviously higher than those in the BC-free particles. In particular, the average SNR for the BC-

180 containing particles is ~2 times those for the BC-free particles in summer and autumn. Such a

181 seasonal variation of SNR is similar to the concentration ratio observed for fine particles in

182 Beijing, with the mean SNR in warmer seasons more than two times in cold seasons [*Li et al.*,

183 2020]. However, the difference of SNRs between the BC-containing and BC-free particles

184 cannot be ruled out based on previous bulk analysis.

185 There is a pronounced diurnal variation of SNRs for the BC-containing particles over the

186 seasons (Fig. 1b). A sharp increase of the SNRs in the BC-containing particles, rather than the

187 BC-free particles, started at noon hour (~12:00). On the other hand, the SNRs of the BC-

188 containing particles decreased from the highest values during the afternoon hours to the lowest

189 contribution during nighttime or early morning. The diurnal trend of SNRs for the BC-

190 containing particles is generally similar to that of temperature (Fig. S4). In both the BC-

191 containing and BC-free particles, nitrate varied in a similar trend, decreasing during the

192 afternoon but increasing during nighttime (Fig. 2), most probably attributed to the

193 heterogeneous uptake of N_2O_5 onto the wet aerosols during high the RH period [*Lee et al.*, 2003;

194 *Wang et al.*, 2009]. The different SNR trends between the BC-containing and BC-free particles

195 could be mainly attributed to the increase of sulfate RPA during the afternoon, specific for the

196 BC-containing particles. Sulfate associated with the BC-free particles does not show a clear

197 trend, but with a distinct afternoon peak in the BC-containing particles (Fig. 2). And thus, the

198   diurnal variation of SNR is most probably driven by the variation of nitrate in the BC-free

199   particles.

200   The diurnal variation of SNRs and BC mixing state is generally consistent with the

201   previously reported data. Distinct diurnal cycles of secondary compositions associated with

202   BC-containing particles in Yangtze River Delta, China [*Wang et al.*, 2016b; *Li et al.*, 2018a],

203   with the increase of sulfate and low volatile oxidized organics in the afternoon due to

204   photochemical oxidation; however, with nitrate peaking during nighttime, driven by

205   thermodynamic equilibria and gas-to-particle partitioning [*Wang et al.*, 2016b]. There are also

206   several studies reporting a correlation between the fraction of internally mixed BC and

207   photochemical activities [*Wang et al.*, 2017; *Xu et al.*, 2018], mainly attributed to the

208   condensation of secondarily formed compositions. Photochemical processing of fresh fractal

209   BC emitted in the early morning to develop a highly aged one, internally mixed with OC,

210   ammonium, sulfate, and nitrate in the afternoon, has been directly observed in Mexico City

211   [*Moffet and Prather*, 2009]. Fast coating of BC was typically found during noontime

212   corresponding to high photochemistry intense and oxidants levels [*Zhang et al.*, 2018; *Liu et*

213   *al.*, 2020]. However, the behavior of BC-free particles has not been reported yet, hindering a

214   further understanding of BC's role in the diurnal variation of SNRs or mixing state.

215   **3.2 Most possible mechanism for the BC-enhanced SNRs**

216   Overall, we found that the SNR for the BC-containing particles is significantly higher than

217   that for the BC-free particles, reflecting a distinct behavior of BC-containing particles towards

218   the formation and evolution of sulfate. The diurnal trend of nitrate and sulfate associated with

219 both the BC-containing and BC-free particles, as discussed above, further indicates that it is the

220 enhanced photochemical formation of sulfate on the BC-containing particles that leads to the

221 higher SNRs. It is the heterogeneous processes that are important since the condensation of

222 gaseous sulfuric and nitric acid gases is expected to be similar for different kinds of particles.

223 The first evidence is the consistent trends between the seasonal and diurnal trends of the SNRs

224 (Fig. 1) and temperature (Fig. S4), which implies a substantial role of photochemistry in the

225 evolution of the BC-containing particles. Compared with the BC-free particles, the role of such

226 chemistry involving BC is evident with a distinctly higher SNR peak in the afternoon hours. In

227 contrast, it seems that the variations of SNRs cannot be simply explained by atmospheric

228 oxidants ($O_x = O_3 + NO_x$) and the trend of their precursors SO_2/NO_x ($R^2 = 0.05$, $p < 0.01$) (Figs.

229 S1 and S3). The second evidence comes from that the increase of SNRs towards higher relative

230 BC content (Fig. S5), indicating that the BC fraction increase might contribute to additional

231 oxidants. The relative importance of these factors, including radiation-related parameters (i.e.,

232 solar radiation and temperature) and the relative BC content in individual particles, in the

233 variation of SNRs for the BC-containing particles, as discussed in section 3.3, further supports

234 the significance of BC-induced photochemistry. As demonstrated by laboratory results,

235 elemental carbon in BC-containing particles can act as a photoactive substrate and has notable

236 catalytic effects on reactions through electronic transfer in the presence of O_2, which produces

237 additional ROS, including $^1O_2$ and $\cdot OH$ [*Li et al.*, 2018b; *Li et al.*, 2019; *Zhu et al.*, 2020].

238 Furthermore, there are also studies reporting the direct contribution of the additional ROS to

239 the formation of sulfate from the oxidation of SO_2 on the surface of BC particles [*Novakov et*

240   *al.*, 1974; *Zhao et al.*, 2017]. And the production could be significantly enhanced with the

241   coexistence of O_3 [*Xu et al.*, 2015; *He et al.*, 2017]. However, the interactions between BC

242   particles and NO_2 unlikely to contribute to the formation of nitrate [*Han et al.*, 2013a; *Guan et*

243   *al.*, 2017].

244   There are also some possible explanations against the above hypothesis but are unlikely to

245   be significant. One is that BC and sulfate or their precursors originate from the same primary

246   sources. This seems unlikely given a relatively low correlation ($R^2 = 0.26$, $p < 0.01$) between

247   the temporal diurnal profiles of the concentration of BC and SO_2. BC is generally produced by

248   incomplete combustion, whereas sulfate is most probably from the secondary process involving

249   the oxidation of its precursor SO_2 [*Xiao et al.*, 2009; *Xue et al.*, 2019], which could be co-

250   emitted with BC. BC is most attributable to the traffic emission in the studied region, with a

251   higher correlation with NO_x ($R^2 = 0.63$, $p < 0.01$), whereas SO_2 or sulfate is mainly produced

252   by coal combustion or biomass burning [*Wang et al.*, 2016c]. Secondly, one may expect that

253   BC facilitates the depletion of nitrate, including evaporation and photochemical degradation.

254   While the additional heat due to the light-absorbing nature of BC may enhance the evaporation

255   of nitrate, our data show that such an effect is limited (Figs. 2 and S4). Although photochemical

256   degradation of nitrate may improve the heterogeneous oxidation of SO_2 through the produced

257   in-particle oxidants (OH, NO_2, and NO_2^-/HNO_2) [*Gen et al.*, 2019; *Zhang et al.*, 2019b], there

258   is still no evidence showing the influence of BC in the photochemistry of nitrate (Fig. S3).

259   Thirdly, higher SNRs associated with BC may also be explained by the fact the freshly emitted

260   smaller BC particles facilitate the condensation of H_2SO_4, due to their larger surface area

261 concentration. However, as shown in Fig. S2, the majority of the BC-containing particles were

262 located in the size range of 0.2-1.0 μm, and extensively mixed with secondary components,

263 which could be regarded as aged particles. More directly, the SNRs show no clear trend with

264 increasing size (Fig. S6), further suggesting the limited influence of particle size on the variation

265 of SNRs.

266   In addition, the role of the transition metals, such as Fe and V, that catalyzed the formation

267 of sulfate [*Ault et al.*, 2010; *Zhang et al.*, 2019a] could be negligible due to their limited number

268 fraction (< 3% on average) and no preferential association with the BC-containing particles. It

269 is also possible that other oxidants (e.g., organic radicals, H_2O_2) play an indispensable role in

270 the evolution of sulfate, yet it is beyond the scope of the present study.

271 **3.3 Factors determining the variations of SNRs**

272   To elucidate the relative importance of various meteorological and chemical factors on the

273 variation of SNRs, multilinear regression is applied to include the most possible influencing

274 factors, i.e., T, RH, O_x, solar radiation (SR), and SO_2/NO_x [*Xu et al.*, 2015; *He et al.*, 2017;

275 *Wang et al.*, 2019a], on the variations of SNRs during the daytime, when the SR data are

276 available. An additional factor, i.e., the relative BC fraction, is added to the regression for the

277 BC-containing particles. As shown in Fig. 3, SNRs in both the BC-containing and BC-free

278 particles could be well explained by these factors, with the evaluation of the model performance

279 provided in Fig. S7. Notably, the variation of the SNRs for the BC-containing particles can be

280 better predicted ($R^2 = 0.68$, $p < 0.01$) by these variables than that for the BC-free particles (R^2

281 $= 0.40$, $p < 0.01$). The addition of the relative BC fraction in the regression improves the

282   correlation coefficient R^2 from 0.54 to 0.68 for the BC-containing particles. An estimation of

283   the relative importance of the predictors shows that the SNRs for the BC-containing particles

284   are mainly dependent on the T (27%), RH (17%), and relative BC content (13%), but with limit

285   dependence on the SO_2/NO_x (2%). Differently, the SNRs for the BC-free particles are

286   dominantly determined by RH (19%), with modest contribution from SO_2/NO_x (7%), O_x (7%),

287   and T (5%).

288   Consistently, random forest analysis could predict ~80% of the SNR variation for the BC-

289   containing particles, and the most important three predictors are T (26%), relative BC content

290   (25%), and RH (17%), as shown in Fig. S8. Since the diurnal variation of T typically tracks the

291   strength of photochemistry [*He et al.*, 2011; *Xu et al.*, 2017], such results further support the

292   importance of photochemistry and the relative BC content in the evolution of sulfate associated

293   with BC. While the analysis may not reliably inform the complex chemical mechanisms of BC

294   involved production of sulfate, the well-fitted results could still indicate the significance of

295   various factors in the variation of SNRs.

296   **3.4 Limitations**

297   The main limitation or bias in the present study is the use of RPA in these qualitative

298   individual mass spectral data rather than the absolute mass concentrations for individual species.

299   It should be noted that it is still quite challenging for the SPAMS based on laser-ablation to

300   provide quantitative information for individual species, due to various uncertainties induced by

301   the laser ionization, such as matrix effects and incomplete ionization [*Jeong et al.*, 2011; *Healy*

302   *et al.*, 2013; *Zhou et al.*, 2016]. Despite this, the variation of RPA is still a good indicator for

303 the investigation of atmospheric processing and mixing state of various particle types, including

304 BC-containing particles, at an individual particle level [*Wang et al.*, 2010; *Zauscher et al.*, 2013;

305 *Zhang et al.*, 2014]. In the present study, even though it is insufficient to provide a quantitative

306 assessment of SNRs on the BC-containing particles, our results do successfully identify a

307 distinct behavior of BC-containing particles in the ambient atmosphere and thus have an

308 advantage of providing a qualitative or semi-quantitative understanding of the evolution of

309 SNRs associated with BC. Future work should target a quantitative understanding of the

310 laboratory kinetics of the photochemical reactions of BC-containing particles, e.g., with

311 Aerodyne SP-AMS.

312 Another limitation is related to identifying the individual BC-containing particles based

313 on the arbitrary defined RPA of carbon ion clusters (i.e., > 0.05). However, as can be seen in

314 Fig. S6, the average SNRs generally increase towards higher relative BC content, regardless of

315 the deviation. It indicates that the methodology for the identification of the BC-containing

316 particles would not lead to an ambiguous conclusion on the distinct behavior of the BC-

317 containing and BC-free particles. While some particle types, including pure ammonium sulfate,

318 and certain organic, cannot simply be ionized by SPAMS, the measured BC-free particles

319 should be still representative of the majority of particle types observed in the urban atmosphere.

320 As shown by microscopic analysis, such pure compounds limitedly contribute to the particle

321 population in a typical urban atmosphere [*Fu et al.*, 2012; *Li et al.*, 2016].

322 **4 Conclusions and Implications**

323   Our results provide observational evidence, extending the laboratory results to the ambient

324   atmosphere that BC could act as a photoactive and absorbing substrate [*Li et al.*, 2018b; *Li et*

325   *al.*, 2019], leading to an enrichment of sulfate. Since there is considerable debate regarding the

326   mechanism for SO_2 oxidation [*Wang et al.*, 2016a; *Xue et al.*, 2016; *Gen et al.*, 2019; *Wang et*

327   *al.*, 2019b; *Wang et al.*, 2020a; *Wang et al.*, 2020c], our finding further underscores the

328   importance of the intrinsic property of BC on the photochemical evolution of sulfate, in

329   particular, during summer and autumn. Given that BC accounts for an essential part of particles

330   in the urban atmosphere [*Ding et al.*, 2016; *Tan et al.*, 2016; *Wang et al.*, 2020b], such a role

331   might be critical for the formation and evolution of sulfate. *Liu et al.* [2019a] observed

332   increasing SNR with altitude over Beijing and attributed the vertical profile to various factors,

333   including plenary boundary layer structure, regional transportation, emission variation, and the

334   aging process of aerosols and gaseous precursors during vertical diffusion. Our analysis may

335   provide an additional explanation associated with photochemistry on the BC-containing

336   particles. The mechanism might also be particularly important during haze episodes when

337   heterogeneous chemistry is thought to play a considerable role in sulfate production [*Zheng et*

338   *al.*, 2015; *Li et al.*, 2020].

339   A most recent chamber simulation reveals that efficient sulfate formation from BC

340   catalyzed SO_2 oxidation in the presence of NO_2 and NH_3 under dark conditions [*Zhang et al.*,

341   2020]. Our evidence further suggests that the photochemical activities during the daytime might

342   also be significant for the production of sulfate and influencing the evolution of BC in the

343   atmosphere. Regarding that sulfate is one of the primary drivers of the BC absorption

344   enhancement in the severely polluted areas in China [*Chen et al.*, 2017], the relative enrichment

345   of sulfate on BC may also partly explain the substantial diurnal variability of light absorption

346   enhancement and single-scattering albedo for BC in eastern China [*Xu et al.*, 2018]. However,

347   the influence of BC on the formation of secondary compositions is rarely considered in models

348   [*Matsui*, 2016], although it is well-known that accounting for variability in per-particle

349   composition and properties would help improve absorption enhancement predictions [*Fierce et*

350   *al.*, 2020]. Therefore, to account for the evolution and climate impact of BC accurately, it is

351   essential to include BC involved photochemistry in the regional aerosol-climate modeling,

352   since the associated sulfate are critical to evaluate the hygroscopic, phase, and optical properties

353   of BC-containing particles [*Ramana et al.*, 2010; *Sun et al.*, 2018; *Liu et al.*, 2019b].

360

361 **Conflict of Interest**

362 There are no conflicts of interest in the article.

363

364 **Data Availability Statement**

365 The processed data supporting this paper are available on Zenodo

366 (10.5281/zenodo.4650206).

367

368 **References**

369 Adachi, K., N. Moteki, Y. Kondo, and Y. Igarashi (2016), Mixing states of light-absorbing

370 particles measured using a transmission electron microscope and a single-particle soot

371 photometer in Tokyo, Japan, *J. Geophys. Res.-Atmos.*, *121*(15), 2016JD025153,

372 doi:10.1002/2016JD025153.

373 Ault, A. P., C. J. Gaston, Y. Wang, G. Dominguez, M. H. Thiemens, and K. A. Prather

374 (2010), Characterization of the Single Particle Mixing State of Individual Ship Plume Events

375 Measured at the Port of Los Angeles, *Environ. Sci. Technol.*, *44*(6), 1954-1961,

376 doi:10.1021/es902985h.

377   Berk, R. A. (2008), Random Forests, in *Statistical Learning from a Regression Perspective*,

378   edited, pp. 1-63, Springer New York, New York, NY, doi:10.1007/978-0-387-77501-2_5.

379   Bond, T. C., et al. (2013), Bounding the role of black carbon in the climate system: A

380   scientific assessment, *J. Geophys. Res.-Atmos.*, *118*(11), 5380-5552, doi:10.1002/Jgrd.50171.

381   Breiman, L. (2001), Random Forests, *Mach. Learn.*, *45*(1), 5-32,

382   doi:10.1023/A:1010933404324.

383   Cahill, J. F., K. Suski, J. H. Seinfeld, R. A. Zaveri, and K. A. Prather (2012), The mixing

384   state of carbonaceous aerosol particles in northern and southern California measured during

385   CARES and CalNex 2010, *Atmos. Chem. Phys.*, *12*(22), 10989-11002, doi:10.5194/acp-12-

386   10989-2012.

387   Chen, B., Z. Zhu, X. Wang, A. Andersson, J. Chen, Q. Zhang, and Ö. Gustafsson (2017),

388   Reconciling modeling with observations of radiative absorption of black carbon aerosols, *J.*

389   *Geophys. Res.-Atmos.*, *122*(11), 5932-5942, doi:10.1002/2017JD026548.

390   Cheng, Y. F., et al. (2009), Influence of soot mixing state on aerosol light absorption and

391   single scattering albedo during air mass aging at a polluted regional site in northeastern China,

392   *J. Geophys. Res.-Atmos.*, *114*(D2), D00G10, doi:10.1029/2008jd010883.

393   Ding, A. J., et al. (2016), Enhanced haze pollution by black carbon in megacities in China,

394   *Geophys. Res. Lett.*, *43*(6), 2873-2879, doi:10.1002/2016GL067745.

395   Fierce, L., et al. (2020), Radiative absorption enhancements by black carbon controlled by

396   particle-to-particle heterogeneity in composition, *Proc. Natl. Acad. Sci. USA*, *117*(10), 5196-

397   5203, doi:10.1073/pnas.1919723117 %J

398   Fu, H., M. Zhang, W. Li, J. Chen, L. Wang, X. Quan, and W. Wang (2012), Morphology,

399   composition and mixing state of individual carbonaceous aerosol in urban Shanghai, *Atmos.*

400   *Chem. Phys.*, *12*(2), 693-707, doi:10.5194/acp-12-693-2012.

401   Gehling, W., and B. Dellinger (2013), Environmentally Persistent Free Radicals and Their

402   Lifetimes in PM2.5, *Environ. Sci. Technol.*, *47*(15), 8172-8178, doi:10.1021/es401767m.

403   Gen, M., R. Zhang, D. D. Huang, Y. Li, and C. K. Chan (2019), Heterogeneous SO2

404   Oxidation in Sulfate Formation by Photolysis of Particulate Nitrate, *Environ. Sci. Tech. Let.*,

405   *6*(2), 86-91, doi:10.1021/acs.estlett.8b00681.

406   Groemping, U. (2006), Relative Importance for Linear Regression in R: The Package

407   relaimpo, *J. Stat. Softw.*, *17*(1), 1-27, doi:10.18637/jss.v017.i01.

408   Gross, D. S., M. E. Galli, P. J. Silva, and K. A. Prather (2000), Relative sensitivity factors

409   for alkali metal and ammonium cations in single particle aerosol time-of-flight mass spectra,

410   *Anal. Chem.*, *72*(2), 416-422.

411   Guan, C., X. Li, W. Zhang, and Z. Huang (2017), Identification of Nitration Products

412   during Heterogeneous Reaction of NO2 on Soot in the Dark and under Simulated Sunlight, *J.*

413   *Phys. Chem. A*, *121*(2), 482-492, doi:10.1021/acs.jpca.6b08982.

414   Han, C., Y. Liu, and H. He (2013a), Heterogeneous photochemical aging of soot by NO2

415   under simulated sunlight, *Atmos. Environ.*, *64*, 270-276, doi:10.1016/j.atmosenv.2012.10.008.

416   Han, C., Y. Liu, and H. He (2013b), Role of Organic Carbon in Heterogeneous Reaction

417   of NO2 with Soot, *Environ. Sci. Technol.*, *47*(7), 3174-3181, doi:10.1021/es304468n.

418   Han, C., Y. C. Liu, J. Z. Ma, and H. He (2012), Key role of organic carbon in the sunlight-

419   enhanced atmospheric aging of soot by O-2, *Proc. Natl. Acad. Sci. USA*, *109*(52), 21250-21255,

420   doi:10.1073/pnas.1212690110.

421   He, C., K. N. Liou, Y. Takano, R. Zhang, M. L. Zamora, P. Yang, Q. Li, and L. R. Leung

422   (2015), Variation of the radiative properties during black carbon aging: theoretical and

423   experimental intercomparison, *Atmos. Chem. Phys.*, *15*(20), 11967-11980, doi:10.5194/acp-15-

424   11967-2015.

425   He, L. Y., X. F. Huang, L. Xue, M. Hu, Y. Lin, J. Zheng, R. Y. Zhang, and Y. H. Zhang

426   (2011), Submicron aerosol analysis and organic source apportionment in an urban atmosphere

427   in Pearl River Delta of China using high-resolution aerosol mass spectrometry, *J. Geophys.*

428   *Res.-Atmos.*, *116*(D12304), 1-15, doi:10.1029/2010jd014566.

429   He, X., S. Pang, J. Ma, and Y. Zhang (2017), Influence of relative humidity on

430   heterogeneous reactions of 03 and O-3/SO2 with soot particles: Potential for environmental and

431   health effects, *Atmos. Environ.*, *165*, 198-206, doi:10.1016/j.atmosenv.2017.06.049.

432   Healy, R. M., et al. (2013), Quantitative determination of carbonaceous particle mixing

433   state in Paris using single-particle mass spectrometer and aerosol mass spectrometer

434   measurements, *Atmos. Chem. Phys.*, *13*(18), 9479-9496, doi:10.5194/acp-13-9479-2013.

435   Healy, R. M., et al. (2012), Sources and mixing state of size-resolved elemental carbon

436   particles in a European megacity: Paris, *Atmos. Chem. Phys.*, *12*(4), 1681-1700,

437   doi:10.5194/acp-12-1681-2012.

438   Huang, X. F., T. L. Sun, L. W. Zeng, G. H. Yu, and S. J. Luan (2012), Black carbon aerosol

439   characterization in a coastal city in South China using a single particle soot photometer, *Atmos.*

440   *Environ.*, *51*, 21-28, doi:10.1016/j.atmosenv.2012.01.056.

441   Jeong, C. H., M. L. McGuire, K. J. Godri, J. G. Slowik, P. J. G. Rehbein, and G. J. Evans

442   (2011), Quantification of aerosol chemical composition using continuous single particle

443   measurements, *Atmos. Chem. Phys.*, *11*(14), 7027-7044, doi:10.5194/acp-11-7027-2011.

444   Khalizov, A. F., M. Cruz-Quinones, and R. Y. Zhang (2010), Heterogeneous Reaction of

445   NO2 on Fresh and Coated Soot Surfaces, *J. Phys. Chem. A*, *114*(28), 7516-7524,

446   doi:10.1021/jp1021938.

447   Kleffmann, J., and P. Wiesen (2005), Heterogeneous conversion of NO2 and NO on HNO3

448   treated soot surfaces: atmospheric implications, *Atmos. Chem. Phys.*, *5*, 77-83,

449   doi:10.5194/acp-5-77-2005.

450   Lee, A. K. Y., M. D. Willis, R. M. Healy, T. B. Onasch, and J. P. D. Abbatt (2015), Mixing

451   state of carbonaceous aerosol in an urban environment: single particle characterization using

452   the soot particle aerosol mass spectrometer (SP-AMS), *Atmos. Chem. Phys.*, *15*(4), 1823-1841,

453   doi:10.5194/acp-15-1823-2015.

454   Lee, S. H., D. M. Murphy, D. S. Thomson, and A. M. Middlebrook (2003), Nitrate and

455   oxidized organic ions in single particle mass spectra during the 1999 Atlanta Supersite Project,

456   *J. Geophys. Res.*, *108*(D7), 8417, doi:10.1029/2001jd001455.

457   Li, K. N., X. N. Ye, H. W. Pang, X. H. Lu, H. Chen, X. F. Wang, X. Yang, J. M. Chen,

458   and Y. J. Chen (2018a), Temporal variations in the hygroscopicity and mixing state of black

459   carbon aerosols in a polluted megacity area, *Atmos. Chem. Phys.*, *18*(20), 15201-15218,

460   doi:10.5194/acp-18-15201-2018.

461   Li, L., et al. (2011), Real time bipolar time-of-flight mass spectrometer for analyzing single

462   aerosol particles, *Intl. J. Mass. Spectrom.*, *303*(2-3), 118-124, doi:10.1016/j.ijms.2011.01.017.

463   Li, M., F. Bao, Y. Zhang, H. Sheng, C. Chen, and J. Zhao (2019), Photochemical Aging

464   of Soot in the Aqueous Phase: Release of Dissolved Black Carbon and the Formation of 1O2,

465   *Environ. Sci. Technol.*, *53*(21), 12311-12319, doi:10.1021/acs.est.9b02773.

466   Li, M., F. Bao, Y. Zhang, W. Song, C. Chen, and J. Zhao (2018b), Role of elemental

467   carbon in the photochemical aging of soot, *Proc. Natl. Acad. Sci. USA*, *115*(30), 7717-7722,

468   doi:10.1073/pnas.1804481115.

469   Li, S., et al. (2020), Characterizing the ratio of nitrate to sulfate in ambient fine particles

470   of urban Beijing during 2018–2019, *Atmos. Environ.*, 117662,

471   doi:https://doi.org/10.1016/j.atmosenv.2020.117662.

472   Li, W. J., L. Y. Shao, D. Z. Zhang, C. U. Ro, M. Hu, X. H. Bi, H. Geng, A. Matsuki, H.

473   Y. Niu, and J. M. Chen (2016), A review of single aerosol particle studies in the atmosphere of

474   East Asia: morphology, mixing state, source, and heterogeneous reactions, *J. Clean. Prod.*, *112*,

475   1330-1349, doi:10.1016/j.jclepro.2015.04.050.

476   Liu, D. T., et al. (2017), Black-carbon absorption enhancement in the atmosphere

477   determined by particle mixing state, *Nature Geosci.*, *10*(3), 184-U132, doi:10.1038/Ngeo2901.

478   Liu, H., X. L. Pan, D. T. Liu, X. Y. Liu, X. S. Chen, Y. Tian, Y. L. Sun, P. Q. Fu, and Z.

479   F. Wang (2020), Mixing characteristics of refractory black carbon aerosols at an urban site in

480   Beijing, *Atmos. Chem. Phys.*, *20*(9), 5771-5785, doi:10.5194/acp-20-5771-2020.

481   Liu, Q., J. Quan, X. Jia, Z. Sun, X. Li, Y. Gao, and Y. Liu (2019a), Vertical Profiles of

482   Aerosol Composition over Beijing, China: Analysis of In Situ Aircraft Measurements, *J. Atmos.*

483   *Sci.*, *76*(1), 231-245, doi:10.1175/JAS-D-18-0157.1 %J Journal of the Atmospheric Sciences.

484   Liu, Y., Z. Wu, X. Huang, H. Shen, Y. Bai, K. Qiao, X. Meng, W. Hu, M. Tang, and L.

485   He (2019b), Aerosol Phase State and Its Link to Chemical Composition and Liquid Water

486   Content in a Subtropical Coastal Megacity, *Environ. Sci. Technol.*, *53*(9), 5027-5033,

487   doi:10.1021/acs.est.9b01196.

488   Matsui, H. (2016), Black carbon simulations using a size- and mixing-state-resolved three-

489   dimensional model: 1. Radiative effects and their uncertainties, *J. Geophys. Res.-Atmos.*, *121*(4),

490   1793-1807, doi:10.1002/2015jd023998.

491   Matsui, H., D. S. Hamilton, and N. M. Mahowald (2018), Black carbon radiative effects

492   highly sensitive to emitted particle size when resolving mixing-state diversity, *Nat. Commun.*,

493   *9*, doi:10.1038/s41467-018-05635-1.

494   McCabe, J., and J. P. D. Abbatt (2009), Heterogeneous Loss of Gas-Phase Ozone on n-

495   Hexane Soot Surfaces: Similar Kinetics to Loss on Other Chemically Unsaturated Solid

496   Surfaces, *J. Phys. Chem. C*, *113*(6), 2120-2127, doi:10.1021/jp806771q.

497   Moffet, R. C., and K. A. Prather (2009), In-situ measurements of the mixing state and

498   optical properties of soot with implications for radiative forcing estimates, *Proc. Natl. Acad.*

499   *Sci. USA*, *106*(29), 11872-11877, doi:10.1073/pnas.0900040106.

500   Motos, G., J. Schmale, J. C. Corbin, M. Zanatta, U. Baltensperger, and M. Gysel-Beer

501   (2019), Droplet activation behaviour of atmospheric black carbon particles in fog as a function

502   of their size and mixing state, *Atmos. Chem. Phys.*, *19*(4), 2183-2207, doi:10.5194/acp-19-

503   2183-2019.

504   Novakov, T., S. G. Chang, and A. B. Harker (1974), Sulfates as Pollution Particulates:

505   Catalytic   Formation   on   Carbon   (Soot)   Particles,   *Science*,   *186*(4160),   259,

506   doi:10.1126/science.186.4160.259.

507   Peng, J. F., et al. (2016), Markedly enhanced absorption and direct radiative forcing of

508   black carbon under polluted urban environments, *Proc. Natl. Acad. Sci. USA*, *113*(16), 4266-

509   4271, doi:10.1073/pnas.1602310113.

510   Penner, J. E. (2019), Soot, sulfate, dust and the climate - three ways through the fog, *Nature*,

511   *570*(7760), 158-159, doi:10.1038/d41586-019-01791-6.

512   Ramana, M. V., V. Ramanathan, Y. Feng, S. C. Yoon, S. W. Kim, G. R. Carmichael, and

513   J. J. Schauer (2010), Warming influenced by the ratio of black carbon to sulphate and the black-

514   carbon source, *Nature Geosci.*, *3*(8), 542-545, doi:10.1038/Ngeo918.

515   Riemer, N., A. P. Ault, M. West, R. L. Craig, and J. H. Curtis (2019), Aerosol Mixing

516   State: Measurements, Modeling, and Impacts, *Rev. Geophys.*, *57*(2), 187-249,

517   doi:10.1029/2018rg000615.

518   Sun, J. X., et al. (2018), Key Role of Nitrate in Phase Transitions of Urban Particles:

519   Implications of Important Reactive Surfaces for Secondary Aerosol Formation, *J. Geophys.*

520   *Res.-Atmos.*, *123*(2), 1234-1243, doi:10.1002/2017JD027264.

521   Tan, H. B., L. Liu, S. J. Fan, F. Li, Y. Yin, M. F. Cai, and P. W. Chan (2016), Aerosol

522   optical properties and mixing state of black carbon in the Pearl River Delta, China, *Atmos.*

523   *Environ.*, *131*, 196-208, doi:10.1016/j.atmosenv.2016.02.003.

524   Wang, G., et al. (2016a), Persistent sulfate formation from London Fog to Chinese haze,

525   *Proc. Natl. Acad. Sci. USA*, *113*(48), 13630, doi:10.1073/pnas.1616540113.

526   Wang, H., et al. (2019a), Aerosols in an arid environment: The role of aerosol water

527   content, particulate acidity, precursors, and relative humidity on secondary inorganic aerosols,

528   *Sci. Total. Environ.*, *646*, 564-572, doi:https://doi.org/10.1016/j.scitotenv.2018.07.321.

529   Wang, J., et al. (2020a), Fast sulfate formation from oxidation of SO2 by NO2 and HONO

530   observed in Beijing haze, *Nat. Commun.*, *11*(1), 2844, doi:10.1038/s41467-020-16683-x.

531   Wang, J., et al. (2017), First Chemical Characterization of Refractory Black Carbon

532   Aerosols and Associated Coatings over the Tibetan Plateau (4730 m a.s.l), *Environ. Sci.*

533   *Technol.*, *51*(24), 14072-14082, doi:10.1021/acs.est.7b03973.

534   Wang, J. F., X. L. Ge, Y. F. Chen, Y. F. Shen, Q. Zhang, Y. L. Sun, J. Z. Xu, S. Ge, H.

535   Yu, and M. D. Chen (2016b), Highly time-resolved urban aerosol characteristics during

536   springtime in Yangtze River Delta, China: insights from soot particle aerosol mass spectrometry,

537   *Atmos. Chem. Phys.*, *16*(14), 9109-9127, doi:10.5194/acp-16-9109-2016.

538   Wang, Q., et al. (2020b), Measurement report: Source and mixing state of black carbon

539   aerosol in the North China Plain: implications for radiative effect, *Atmos. Chem. Phys.*, *20*(23),

540   15427-15442, doi:10.5194/acp-20-15427-2020.

541   Wang, Q. Y., et al. (2016c), Physicochemical characteristics of black carbon aerosol and

542   its radiative impact in a polluted urban area of China, *J. Geophys. Res.-Atmos.*, *121*(20), 12505-

543   12519, doi:10.1002/2016jd024748.

544   Wang, S., S. Zhou, Y. Tao, W. G. Tsui, J. Ye, J. Z. Yu, J. G. Murphy, V. F. McNeill, J. P.

545   D. Abbatt, and A. W. H. Chan (2019b), Organic Peroxides and Sulfur Dioxide in Aerosol:

546   Source of Particulate Sulfate, *Environ. Sci. Technol.*, doi:10.1021/acs.est.9b02591.

547   Wang, X., et al. (2020c), Atmospheric Photosensitization: A New Pathway for Sulfate

548   Formation, *Environ. Sci. Technol.*, doi:10.1021/acs.est.9b06347.

549   Wang, X. F., S. Gao, X. Yang, H. Chen, J. M. Chen, G. S. Zhuang, J. D. Surratt, M. N.

550   Chan, and J. H. Seinfeld (2010), Evidence for High Molecular Weight Nitrogen-Containing

551   Organic Salts in Urban Aerosols, *Environ. Sci. Technol.*, *44*(12), 4441-4446.

552   Wang, X. F., Y. P. Zhang, H. Chen, X. Yang, J. M. Chen, and F. H. Geng (2009),

553   Particulate Nitrate Formation in a Highly Polluted Urban Area: A Case Study by Single-Particle

554   Mass   Spectrometry   in   Shanghai,   *Environ.   Sci.   Technol.*,   *43*(9),   3061-3066,

555   doi:10.1021/es8020155.

556   Xiao, R., et al. (2009), Formation of submicron sulfate and organic aerosols in the outflow

557   from the urban region of the Pearl River Delta in China, *Atmos. Environ.*, *43*(24), 3754-3763.

558   Xu, W., et al. (2017), Effects of Aqueous-Phase and Photochemical Processing on

559   Secondary Organic Aerosol Formation and Evolution in Beijing, China, *Environ. Sci. Technol.*,

560   *51*(2), 762-770, doi:10.1021/acs.est.6b04498.

561   Xu, W., Q. Li, J. Shang, J. Liu, X. Feng, and T. Zhu (2015), Heterogeneous oxidation of

562   SO2 by O3-aged black carbon and its dithiothreitol oxidative potential, *J. Environ. Sci.*, *36*, 56-

563   62, doi:https://doi.org/10.1016/j.jes.2015.02.014.

564 Xu, X. Z., et al. (2018), The influence of photochemical aging on light absorption of
565 atmospheric black carbon and aerosol single-scattering albedo, *Atmos. Chem. Phys.*, *18*(23),
566 16829-16844, doi:10.5194/acp-18-16829-2018.

567 Xue, J., X. Yu, Z. Yuan, S. M. Griffith, A. K. H. Lau, J. H. Seinfeld, and J. Z. Yu (2019),
568 Efficient control of atmospheric sulfate production based on three formation regimes, *Nature*
569 *Geosci.*, *12*(12), 977-982, doi:10.1038/s41561-019-0485-5.

570 Xue, J., Z. Yuan, S. M. Griffith, X. Yu, A. K. H. Lau, and J. Z. Yu (2016), Sulfate
571 Formation Enhanced by a Cocktail of High NOx, SO2, Particulate Matter, and Droplet pH
572 during Haze-Fog Events in Megacities in China: An Observation-Based Modeling Investigation,
573 *Environ. Sci. Technol.*, *50*(14), 7325-7334, doi:10.1021/acs.est.6b00768.

574 Yu, C. J., D. T. Liu, K. Broda, R. Joshi, J. Olfert, Y. L. Sun, P. Q. Fu, H. Coe, and J. D.
575 Allan (2020), Characterising mass-resolved mixing state of black carbon in Beijing using a
576 morphology-independent measurement method, *Atmos. Chem. Phys.*, *20*(6), 3645-3661,
577 doi:10.5194/acp-20-3645-2020.

578 Yuan, Q., J. Xu, Y. Wang, X. Zhang, Y. Pang, L. Liu, L. Bi, S. Kang, and W. Li (2019),
579 Mixing State and Fractal Dimension of Soot Particles at a Remote Site in the Southeastern
580 Tibetan Plateau, *Environ. Sci. Technol.*, *53*(14), 8227-8234, doi:10.1021/acs.est.9b01917.

581 Zauscher, M. D., Y. Wang, M. J. K. Moore, C. J. Gaston, and K. A. Prather (2013), Air
582 Quality Impact and Physicochemical Aging of Biomass Burning Aerosols during the 2007 San
583 Diego Wildfires, *Environ. Sci. Technol.*, *47*(14), 7633-7643, doi:10.1021/es4004137.

584 Zhang, F., et al. (2020), An unexpected catalyst dominates formation and radiative forcing
585 of regional haze, *Proc. Natl. Acad. Sci. USA*, *117*(8), 3960-3966, doi:10.1073/pnas.1919343117.

586 Zhang, G., et al. (2017), The single-particle mixing state and cloud scavenging of black
587 carbon: a case study at a high-altitude mountain site in southern China, *Atmos. Chem. Phys.*,
588 *17*(24), 14975-14985, doi:10.5194/acp-17-14975-2017.

589 Zhang, G., et al. (2019a), Oxalate Formation Enhanced by Fe-Containing Particles and
590 Environmental Implications, *Environ. Sci. Technol.*, *53*(3), 1269-1277,
591 doi:10.1021/acs.est.8b05280.

592   Zhang, G. H., X. H. Bi, J. J. He, D. H. Chen, L. Y. Chan, G. W. Xie, X. M. Wang, G. Y.

593   Sheng, J. M. Fu, and Z. Zhou (2014), Variation of secondary coatings associated with elemental

594   carbon by single particle analysis, *Atmos. Environ.*, *92*, 162-170,

595   doi:10.1016/j.atmosenv.2014.04.018.

596   Zhang, G. H., X. H. Bi, L. Li, L. Y. Chan, M. Li, X. M. Wang, G. Y. Sheng, J. M. Fu, and

597   Z. Zhou (2013), Mixing state of individual submicron carbon-containing particles during spring

598   and fall seasons in urban Guangzhou, China: a case study, *Atmos. Chem. Phys.*, *13*(9), 4723-

599   4735, doi:10.5194/acp-13-4723-2013.

600   Zhang, R. Y., A. F. Khalizov, J. Pagels, D. Zhang, H. X. Xue, and P. H. McMurry (2008),

601   Variability in morphology, hygroscopicity, and optical properties of soot aerosols during

602   atmospheric processing, *Proc. Natl. Acad. Sci. USA*, *105*(30), 10291-10296,

603   doi:10.1073/pnas.0804860105.

604   Zhang, Y., F. Bao, M. Li, C. Chen, and J. Zhao (2019b), Nitrate-Enhanced Oxidation of

605   SO2 on Mineral Dust: A Vital Role of a Proton, *Environ. Sci. Technol.*, *53*(17), 10139-10145,

606   doi:10.1021/acs.est.9b01921.

607   Zhang, Y., et al. (2018), Sizing of Ambient Particles From a Single-Particle Soot

608   Photometer Measurement to Retrieve Mixing State of Black Carbon at a Regional Site of the

609   North China Plain, *J. Geophys. Res.-Atmos.*, *123*(22), 12778-12795,

610   doi:10.1029/2018jd028810.

611   Zhao, Y., Y. Liu, J. Ma, Q. Ma, and H. He (2017), Heterogeneous reaction of SO2 with

612   soot: The roles of relative humidity and surface composition of soot in surface sulfate formation,

613   *Atmos. Environ.*, *152*, 465-476, doi:http://dx.doi.org/10.1016/j.atmosenv.2017.01.005.

614   Zheng, B., Q. Zhang, Y. Zhang, K. B. He, K. Wang, G. J. Zheng, F. K. Duan, Y. L. Ma,

615   and T. Kimoto (2015), Heterogeneous chemistry: a mechanism missing in current models to

616   explain secondary inorganic aerosol formation during the January 2013 haze episode in North

617   China, *Atmos. Chem. Phys.*, *15*(4), 2031-2049, doi:10.5194/acp-15-2031-2015.

618   Zhou, Y., et al. (2016), A field measurement based scaling approach for quantification of

619   major ions, organic carbon, and elemental carbon using a single particle aerosol mass

620   spectrometer, *Atmos. Environ.*, *143*, 300-312, doi:10.1016/j.atmosenv.2016.08.054.

621   Zhu, J., J. Shang, Y. Chen, Y. Kuang, and T. Zhu (2020), Reactive Oxygen Species-

622   Related Inside-to-Outside Oxidation of Soot Particles Triggered by Visible-Light Irradiation:

623   Physicochemical Property Changes and Oxidative Potential Enhancement, *Environ. Sci.*
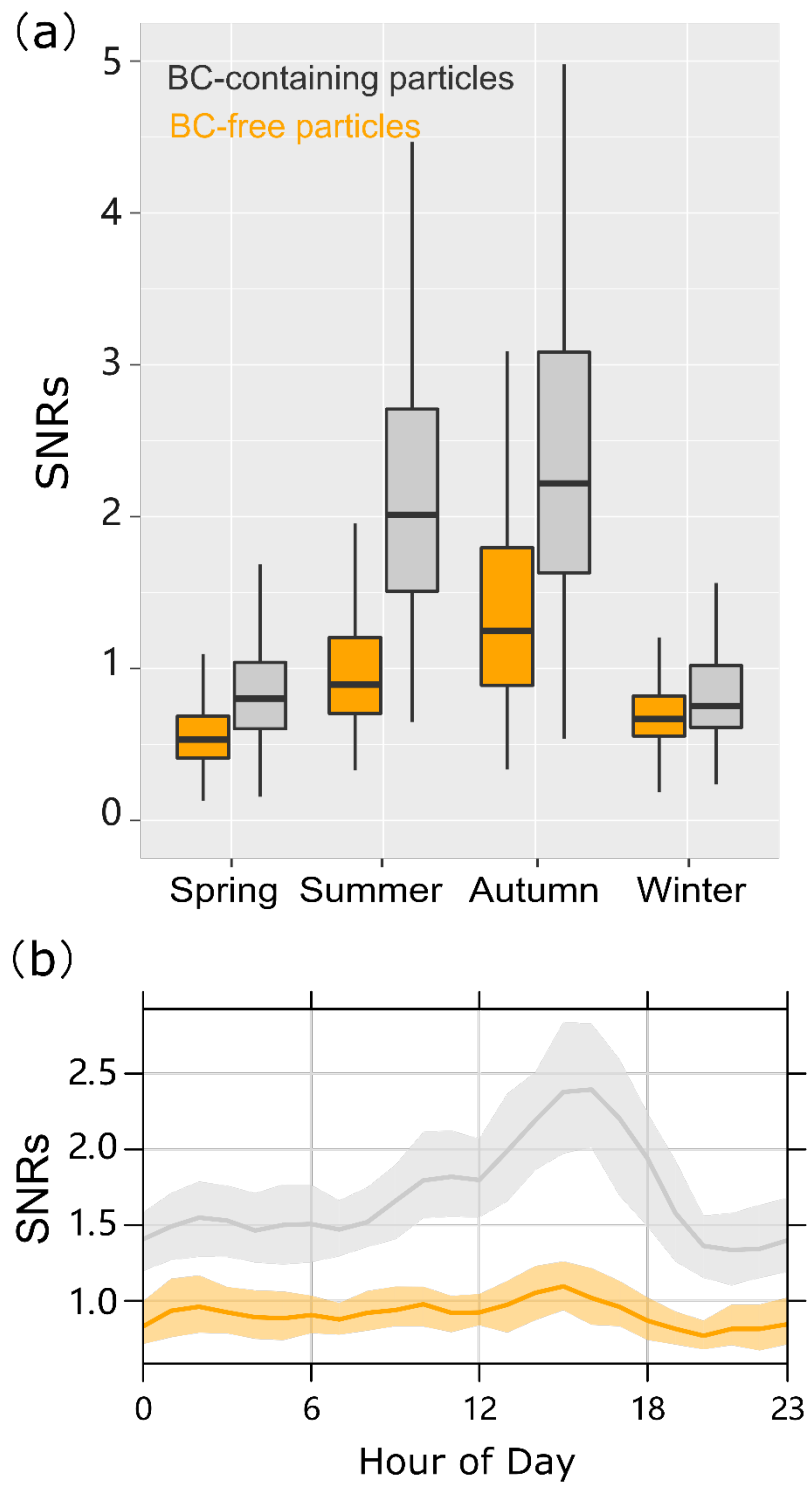
624   *Technol.*, doi:10.1021/acs.est.0c01150.

625

Figure Caption

627 **Figure 1.** (a) Seasonal variation of SNRs for the BC-containing and BC-free particles,

628 respectively. Box and whisker plot shows lower, median, and upper lines, denoting

629 the 25th, 50th, and 75th percentiles, respectively; the lower and upper edges denote

630 the 10th and 90th percentiles, respectively. (b) Diurnal variation of SNRs for the BC-

631 containing and BC-free particles, respectively. The shadings indicate the 95%

632 confidence intervals of the hourly mean values.

633 **Figure 2.** The diurnal trends of sulfate and nitrate RPA in the (a) BC-containing and

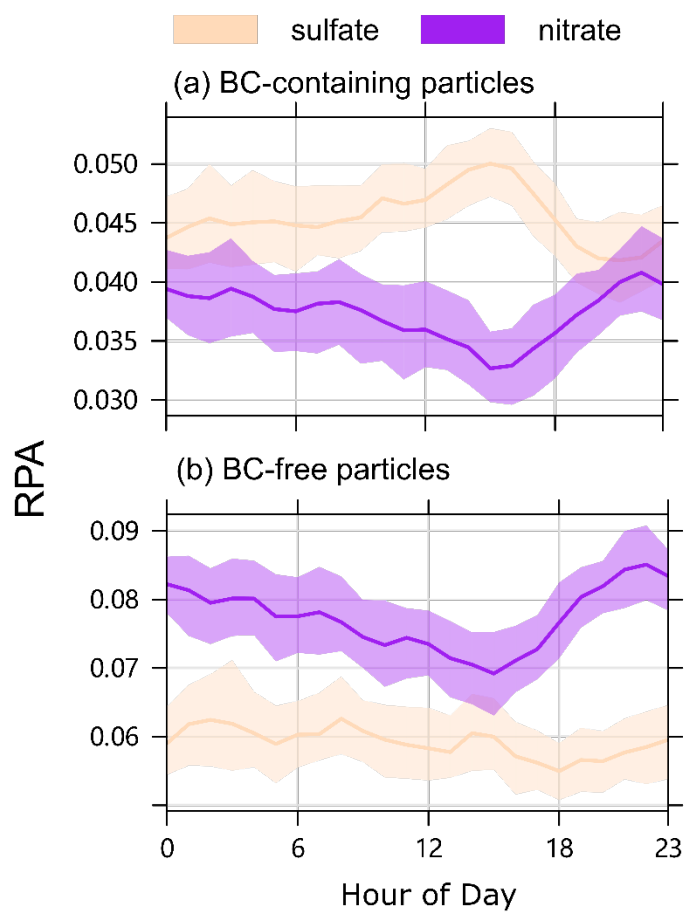634 (b) BC-free particles, respectively.

635 **Figure 3.** Comparison between the measured and regressed SNRs, and the relative

636 importance of various factors on the variations of SNRs for the (a and c) BC-

637 containing and (b and d) BC-free particles, respectively. The shadings for the

638 regressed line (a and b) indicate the 95% confidence intervals. The error bars (in c and

639 d) provide confidence intervals for the relative importance with 100 bootstrap
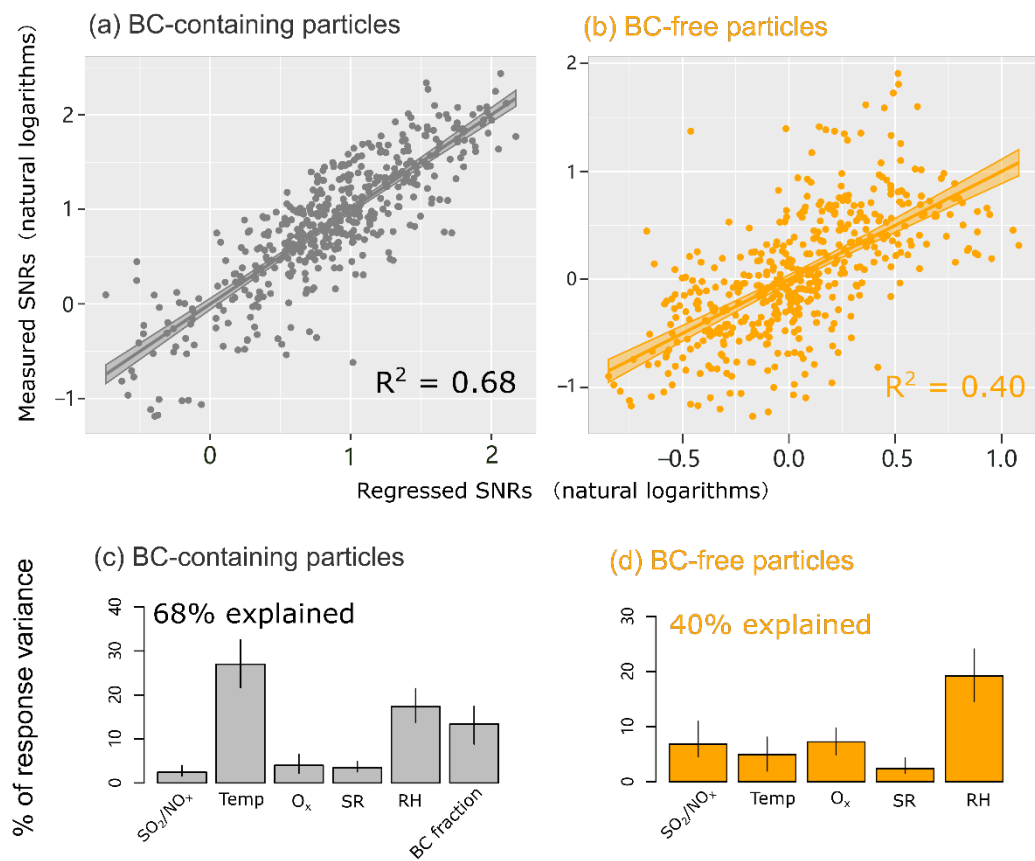
640 replicates to evaluate the results.

641

642

Fig. 1.

644

Fig. 2.

(a) BC-containing particles

(b) BC-free particles

(c) BC-containing particles

(d) BC-free particles

646

647   Fig. 3.